Aluminum-Calcium Composite Conductors: The Future of America's Power Grid

Jennifer Lew
Palos Verdes Peninsula High School
Rancho Palos Verdes, USA
jenniferlew2004@gmail.com

***Abstract*—To lower the cost of transmission line construction and increase the viability of renewable energy projects, the current research investigates the cost benefits of replacing Aluminum Conductor Steel Reinforced (ACSR) conductors with Aluminum-Calcium Composite (Al-Ca) conductors. The research modeled the conductivity of both conductors at frequencies of 0 Hz, 50 Hz, and 60 Hz. In all cases, regardless of conductor diameter, the research found that Al-Ca conductor displayed superior conductivity versus ACSR. With greater conductivity, circuits made of Al-Ca would experience less power loss from resistive heating. In addition, the research found that the superior yield strength of Al-Ca allowed for longer span lengths; consequently, a transmission circuit built using Al-Ca would require fewer support towers than the same circuit built using ACSR. As support towers can comprise as much as half of construction costs, using Al-Ca can lead to significant savings.**

***Index Terms*—Al-Ca, ACSR, impedance, conductor, conductivity, composite, power transmission**

I. Introduction

As America moves to renewable energy, the construction of transmission lines will increase. California recently completed the 250-mile Tehachapi Renewable Transmission Project (TRTP) to bring wind energy to Los Angeles County. Although renewable energy has numerous benefits, such projects have high costs ($2.5 billion for TRTP). Thus, lowering the cost of transmission line facilities will accelerate the rollout of renewable energy. The research analyzes the benefits of replacing transmission conductors - namely Aluminum Conductor Steel Reinforced (ACSR) - with Aluminum-Calcium Composite Conductor (Al-Ca). Al-Ca has a conductivity equal to 95% of pure aluminum, yet has twice the yield strength of ACSR. Due to its strength, Al-Ca can be built with longer span lengths, thereby decreasing the requisite number of support towers.

II. Theoretical Approach

A. Modeling the Conductor

To compare ACSR to Al-Ca, a model must be created to calculate the conductor current density, J, and impedance, Z. ACSR, which is composed of a steel core with an outer layer of aluminum, is inhomogeneous while Al-Ca is homogeneous. A model that is appropriate for both types of conductors involves dividing the conductor cross-section into circular layers - where each layer is homogeneous - and calculating the current density in each layer. Dividing the cross-section into m layers will result in one cylindrical conductor at the center and $m-1$ tubular conductors. This layering method is shown in Figure 1, where n represents the index of the associated layer.

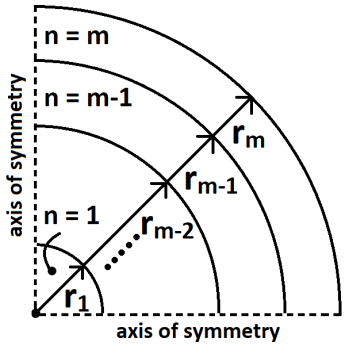

Fig. 1. Model of a conductor cross-section showing layering methodology.

B. Calculating the Electrical Properties of a Conductor

The outermost layer, Layer m, has an outer and inner radius of $r = r_m$ and $r = r_{m-1}$, respectively. If the conductor has an overall radius of R, then $r_m = R$. The next layer, Layer $m-1$, would have an outer and inner radius of $r = r_{m-1}$ and $r = r_{m-2}$, respectively. Continuing this pattern, the innermost layer, i.e. the cylindrical conductor at the very center, has an outer and inner radius of $r = r_1$ and $r = 0$, respectively. With n as the index associated with the layers, it can be shown that the electric and magnetic field at the outer radius of a Layer n, denoted as $E(r_n)$ and $H(r_n)$, respectively, is related to the electric and magnetic field at the outer radius of Layer $n-1$, denoted as $E(r_{n-1})$ and $H(r_{n-1})$, respectively, by the following equation:

$$\begin{bmatrix} E(r_n) \\ H(r_n) \end{bmatrix} = \begin{bmatrix} a_n & b_n \\ c_n & d_n \end{bmatrix} \cdot \begin{bmatrix} E(r_{n-1}) \\ H(r_{n-1}) \end{bmatrix} \quad (1)$$

where:

$$a_n = \frac{\pi z_{n-1}}{2}\left[-J_0(z_n)Y_1(z_{n-1}) + J_1(z_{n-1})Y_0(z_n)\right] \quad (2)$$

$$b_n = j\omega\frac{\mu_n}{k_n}\frac{\pi z_{n-1}}{2}[-J_0(z_n)Y_0(z_{n-1}) + J_0(z_{n-1})Y_0(z_n)] \quad (3)$$

978-1-7281-7571-3/20/$31.00 ©2020 IEEE

$$c_n = \frac{j}{\omega}\frac{\pi z_{n-1}}{2}\frac{k_n}{\mu_n}[-J_1(z_n)Y_1(z_{n-1}) + J_1(z_{n-1})Y_1(z_n)] \quad (4)$$

$$d_n = \frac{\pi z_{n-1}}{2}\left[J_1(z_n)Y_0(z_{n-1}) - J_0(z_{n-1})Y_1(z_n)\right] \quad (5)$$

$$k_n = \sqrt{-j\omega\mu_n\sigma_n} \quad (6)$$

$$z_n = k_n r_n \quad (7)$$

In (2) through (7), k_n is the wavenumber of the n^{th} layer; μ_n is the magnetic permeability of the n^{th} layer; σ_n is the electrical conductivity of the n^{th} layer; ω is the angular frequency of the electric current; J_0 is the Bessel function of the first kind of order 0; J_1 is the Bessel function of the first kind of order 1; Y_0 is the Bessel function of the second kind of order 0; Y_1 is the Bessel function of the second kind of order 1. Consequently, a_n, b_n, c_n, and d_n are values that uniquely describe the properties of a particular Layer n. The method of transmission matrices in (1) can be used to find the electric and magnetic field in any layer as long as the electric and magnetic field of the inner adjacent layer is known. This means that, ultimately, the field in every layer can be found by simply determining two values: $E(r_1)$ and $H(r_1)$, i.e. the electric and magnetic field of the solid cylinder at the center of the conductor. If the conductor is homogeneous (such that every layer shares the same k and σ values), then we can use the known result for the electric and magnetic fields within a homogeneous conductor:

$$E(r_1) = I\frac{k}{2\pi R\sigma}\frac{J_0(kr_1)}{J_1(kR)} \quad (8)$$

$$H(r_1) = \frac{I}{2\pi R}\frac{J_1(kr_1)}{J_1(kR)} \quad (9)$$

where I is the current on the conductor in amperes. If the conductor is inhomogeneous, then $E(r_1)$ and $H(r_1)$ must be calculated using the wavenumber and conductivity value specific to Layer 1:

$$E(r_1) = I\frac{k_1}{2\pi R\sigma_1}\frac{J_0(k_1r_1)}{J_1(k_1R)} \quad (10)$$

$$H(r_1) = \frac{I}{2\pi R}\frac{J_1(k_1r_1)}{J_1(k_1R)} \quad (11)$$

After solving for $E(r_1)$ and $H(r_1)$, $E(r_n)$ and $H(r_n)$ of any Layer n can be found by performing a series of $n-1$ matrix multiplications using (1) to yield:

$$\begin{bmatrix} E(r_n) \\ H(r_n) \end{bmatrix} = \begin{bmatrix} a & b \\ c & d \end{bmatrix} \cdot \begin{bmatrix} E(r_1) \\ H(r_1) \end{bmatrix} \quad (12)$$

Specifically, $E(r_n)$ and $H(r_n)$ is calculated as:

$$E(r_n) = aE(r_1) + bH(r_1) \quad (13)$$

$$H(r_n) = cE(r_1) + dH(r_1) \quad (14)$$

In (13) and (14), it should be noted that the values a, b, c, d are composite numbers that result from multiple matrix multiplications. At this point, for a homogeneous conductor, the current density J_n in any Layer n can be found by multiplying the real part of the electric field in that layer to the conductivity value:

$$J_n = \sigma Re\{E(r_n)\} \quad (15)$$

For an inhomogeneous conductor, the current density J_n in any Layer n can be found by multiplying the real part of the electric field in that layer to the conductivity value specific to that layer:

$$J_n = \sigma_n Re\{E(r_n)\} \quad (16)$$

Finally, the conductor impedance Z can be determined by following a similar path; first, the surface impedance of the inner cylindrical conductor, i.e. Layer 1, is calculated:

$$Z(r_1) = \frac{\omega\mu_1}{jk_1}\frac{J_0(k_1r_1)}{J_1(k_1r_1)} \quad (17)$$

The surface impedance of Layer 1 given in (17) can be translated to find the overall surface impedance of the whole conductor as follows:

$$Z(r_n) = \frac{aZ(r_1) + b}{cZ(r_1) + d} \quad (18)$$

In (18), it is understood that a, b, c, and d are composite values that result from using (12) to calculate the electric and magnetic field of the outermost layer, i.e. $E(r_m)$ and $H(r_m)$. The conductor impedance Z, i.e. the overall internal impedance of the whole conductor, can then be found:

$$Z = \frac{Z(r_n)}{2\pi R} \quad (19)$$

At this point, two caveats regarding the above calculations must be made. First, (10) and (11) do not produce accurate values because formulas intended for homogeneous conductors cannot be used for inhomogeneous conductors. In the case of ACSR, (10) and (11) will produce overestimated values, leading (16) to overestimate the current density J_n. But this can be corrected by scaling down the value of I in (10) and (11) until the current density using (16), integrated over the entire conductor cross section, reproduces the expected value of I. Second, Bessel functions produce erroneous results when their arguments become too large. Therefore, the above equations will lose accuracy for large conductor diameters, as shown in [1].

III. Electromagnetic Simulations to Determine Conductor Impedance

A. Simulation Setup

The most common ACSR conductors are composed of 6 Al strands and 1 steel strand ("6/1") or 26 Al strands and 7 steel strands ("26/7"). In the former, steel comprises 14.2% of the total cross-sectional area; in the latter, steel comprises 15.9% of the total cross-sectional area. In the current research, the two types of ACSR will be modeled as completely solid conductors with the aforementioned amount of steel. Similarly, Al-Ca will also be modeled as a solid conductor. As a result,

the effect of the interstitial spaces due to stranding will be ignored, as was done in [2]. This is appropriate for the current research, as the aim of the research is to quantify the relative difference in impedance and conductivity between ACSR and Al-Ca and not to calculate the actual values. The simulation consists of applying a current of 1 ampere on the conductor at a frequency f of 60 Hz, 50 Hz, and 0 Hz (DC), which are the most common power transmission frequencies. For Al-Ca, the conductivity and relative magnetic permeability is σ = 3.302E7 m/Ω-m^2 and μ_r = 1, respectively, per [3]; for aluminum, these two values are σ = 3.500E7 m/Ω-m^2 and μ_r = 1; for steel, these two values are σ = 1.450E6 m/Ω-m^2 and μ_r = 70.

B. Results

The simulation, using the previously described matrix methodology, was performed in Python. The resulting impedance values of Al-Ca, 14.2% steel ACSR, and 15.9% steel ACSR are shown in Table I. The results show that, given the same overall diameter, conductors comprised of Al-Ca consistently exhibit lower impedance than ACSR. Table II uses the impedance values from Table I to calculate the percent improvement in conductivity of Al-Ca over ACSR. Across the conductor diameters and frequencies tested, Al-Ca has 9.24% to 11.43% greater conductivity than ACSR. The superior conductivity of Al-Ca over ACSR is attributable to the general absence of the skin effect: due to the low operating frequency and small conductor diameter, there will be current flow across the entire conductor cross-section; for ACSR, this means that current is forced to flow on the much less conductive steel portion of the conductor. Figures 2 and 3 are current density distribution polar plots generated from the Python simulation. Figure 2, which depicts Al-Ca, shows relatively even current density throughout the entire conductor cross-section; the current density ranges from $J \approx 5205 A/m^2$ to $J \approx 5275 A/m^2$. Figure 3, which depicts ACSR, shows relatively even current density throughout the aluminum cross-section of $J \approx 6000 A/m^2$ and throughout the steel cross-section of less than $J \approx 1000 A/m^2$

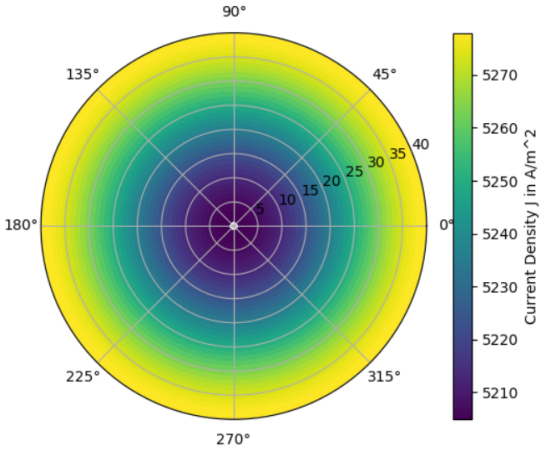

Fig. 2. Current density distribution polar plot for 0.6129 inch diameter Al-Ca with a current of 1 ampere at 60 Hz.

TABLE I
IMPEDANCE[a] (Z) OF AL-CA AND ACSR[b] AT FREQUENCIES OF 60 HZ, 50 HZ, AND 0 HZ

Impedance of Al-Ca			
Diameter (inch)	***f = 60 Hz***	***f = 50 Hz***	***f = 0 Hz***
0.2043	0.4365+0.0058j	0.4365+0.0048j	0.4365
0.4086	0.1092+0.0057j	0.1092+0.0048j	0.1091
0.6129	0.0487+0.0057j	0.0487+0.0048j	0.0485
0.8172	0.0277+0.0057j	0.0276+0.0048j	0.0273
1.0215	0.0181+0.0056j	0.0179+0.0047j	0.0175
Impedance of ACSR (14.3% steel by area)			
Diameter (inch)	***f = 60 Hz***	***f = 50 Hz***	***f = 0 Hz***
0.2043	0.4779+0.0045j	0.4779+0.0038j	0.4779
0.4086	0.1195+0.0045j	0.1195+0.0038j	0.1195
0.6129	0.0532+0.0045j	0.0532+0.0038j	0.0531
0.8172	0.0301+0.0045j	0.0300+0.0038j	0.0299
1.0215	0.0194+0.0045j	0.0193+0.0037j	0.0191
Impedance of ACSR (15.9% steel by area)			
Diameter (inch)	***f = 60 Hz***	***f = 50 Hz***	***f = 0 Hz***
0.2043	0.4864+0.0044j	0.4864+0.0037j	0.4864
0.4086	0.1216+0.0044j	0.1216+0.0037j	0.1216
0.6129	0.0541+0.0044j	0.0541+0.0037j	0.0540
0.8172	0.0306+0.0044j	0.0305+0.0037j	0.0304
1.0215	0.0197+0.0044j	0.0197+0.0037j	0.0195

[a]Impedance per 1000 feet of conductor.
[b]ACSR is modeled as a solid conductor with no interstitial spaces.

TABLE II
PERCENT IMPROVEMENT IN CONDUCTIVITY OF AL-CA OVER ACSR AT FREQUENCIES OF 60 HZ, 50 HZ, AND 0 HZ

f = 60 Hz		
Diameter (inch)	***ACSR (14.3% steel)***	***ACSR (15.9% steel)***
0.2043	9.50%	11.43%
0.4086	9.44%	11.37%
0.6129	9.22%	11.12%
0.8172	8.63%	10.48%
1.0215	7.47%	9.24%
f = 50 Hz		
Diameter (inch)	***ACSR (14.3% steel)***	***ACSR (15.9% steel)***
0.2043	9.50%	11.43%
0.4086	9.46%	11.39%
0.6129	9.31%	11.22%
0.8172	8.89%	10.78%
1.0215	8.05%	9.84%
f = 0 Hz		
Diameter (inch)	***ACSR (14.3% steel)***	***ACSR (15.9% steel)***
0.2043	9.50%	11.43%
0.4086	9.50%	11.44%
0.6129	9.48%	11.42%
0.8172	9.49%	11.44%
1.0215	9.51%	11.40%

IV. MECHANICAL CALCULATIONS TO DETERMINE MAXIMUM ALLOWABLE SPAN LENGTHS

Because Al-Ca is both stronger and lighter than ACSR, Al-Ca conductors can be strung with longer span lengths (defined as the straight line distance between the two towers on which the conductor is supported). To see the difference in the maximum allowable span length, the research proposes the following experiment: a size "636" 26/7 ACSR conductor will be strung at a span length, S, that yields a mid-span sag, ϵ of 25 feet and a tension, T, equal to 20% of its rated breaking strength; the experiment will then be repeated for an Al-Ca

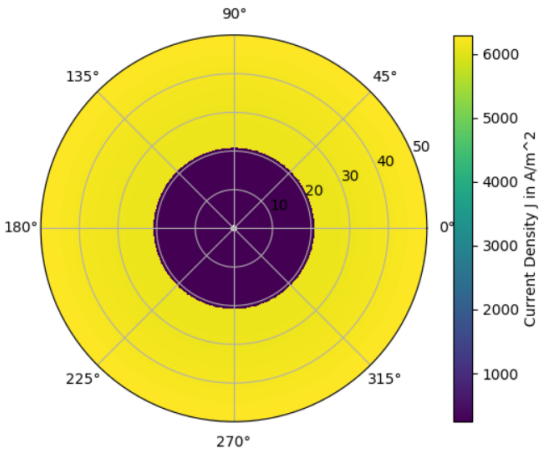

Fig. 3. Current density distribution polar plot for 0.6129 inch diameter ACSR (15.9% steel) with a current of 1 ampere at 60 Hz.

conductor of equivalent cross-sectional area. This experiment setup is shown in Figure 4.

A. Tension Calculations with Known Conductor Sag

If both ends of a conductor are supported at the same height, an initial guess for the curvature a (in feet) of the conductor is:

$$a \approx \frac{S^2 + 4\epsilon^2}{8\epsilon} \tag{20}$$

The calculated sag ϵ is:

$$\epsilon = acosh\left(\frac{0.5S}{a}\right) - a \tag{21}$$

The exact value for curvature can be found by adjusting a until (21) matches the known conductor sag. The tension in the conductor can then be found:

$$T = \rho\sqrt{a^2 + \left(\frac{S}{2}\right)^2} \tag{22}$$

In (22), ρ is the conductor weight density in pound per foot.

B. Results

The results in Table III show that, given a required sag of 25 feet, "636" 26/7 ACSR can achieve a span length of 1075 feet before reaching 20% of its rated strength; Al-Ca, on the other hand, can achieve a span length of 1710 feet before reaching 20% of its rated strength. As a result, a transmission circuit comprised mainly of Al-Ca may require 35% fewer transmission towers as compared to a transmission circuit comprised of ACSR.

V. Conclusion

The research has shown that across a range of conductor diameters and frequencies, Al-Ca conductors are approximately 10% more conductive than ACSR conductors of the same cross-sectional area. This indicates that replacing ACSR with Al-Ca can lead to less power loss from resistive heating. California alone loses $2.5 billion a year due to such losses;

TABLE III
Comparison of the Maximum Allowable Span Length for ACSR and Al-Ca

	Size 636, 26/7 ACSR	***Al-Ca***[a]
weight density (lb/ft)	0.874	0.694
Span length (ft)	1075	1710
Required sag (ft)	25	25
Curvature (ft)	5782	14623
Tension (lb)	5075	10166
Rated strength (lb)	25200	50400
% of Rated strength	20.14%	20.17%

[a]Al-Ca conductor of equivalent cross-sectional area.

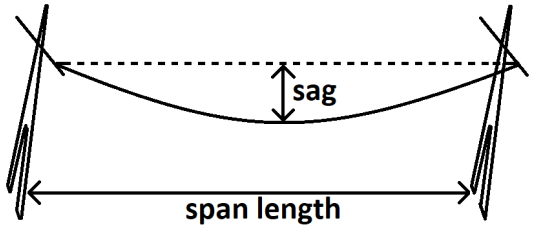

Fig. 4. A conductor span supported by two transmission towers.

as such, a 10% increase in conductivity can yield annual savings of $0.25 billion. Additionally, due to the greater span length capability of Al-Ca, a transmission circuit can have approximately 35% fewer transmission towers (all else being equal). This efficiency in construction would lead to additional billions in savings and increase the viability of renewable energy projects. In turn, these new sources of renewable energy can replace old sources of dirty energy such as natural gas and coal. The progress made in these endeavors can dramatically slow or potentially stop climate change.

Acknowledgment

The author is thankful for the assistance of Derek Fong, PE, Senior Utilities Engineer Supervisor at the California Public Utilities Commission (CPUC). The CPUC is an agency tasked with regulating electric, gas, and communications utilities in the State of California. Based on information received via correspondences with the aforementioned engineer, the author was able to understand the complexities and nuances of electromagnetic theory, software development, and their application to power systems.

References

[1] Vedran Boras, Slavko Vujevic, Dino Lovric, "Definition and computation of cylindrical conductor internal impedance for large parameters", Applied Electromagnetics and Communications (ICECom) International Conference on, 2010.

[2] Karolina Kasaš-Lažetić, Dejana Herceg, Dragan Kljajić, Gorana Mijatović, Miroslav Prša, "Impact of steel permeability on ACSR impedance per unit length", Industrial Electronics (INDEL) International Symposium on, pp. 1-4, 2016.

[3] Liang Tian, Alan Russell, Trevor Riedemann, Soeren Mueller, Iver Anderson, "A deformation-processed Al-matrix/Ca-nanofilamentary composite with low density, high strength, and high conductivity", Materials Science and Engineering, pp. 348-354, 2017.